

Measuring gravitational effect of superintense laser by spin-squeezed Bose–Einstein condensates interferometer

Eng Boon Ng† and C. H. Raymond Ooi‡

Citation: Chin. Phys. B, 2022, 31 (**5**): 053701. DOI: 10.1088/1674-1056/ac4231
Journal homepage: http://cpb.iphy.ac.cn; http://iopscience.iop.org/cpb

What follows is a list of articles you may be interested in

Interference properties of a trapped atom interferometer in two asymmetric optical dipole traps

Li-Yong Wang(王立勇), Xiao Li(李潇), Kun-Peng Wang(王坤鹏), Yin-Xue Zhao(赵吟雪), Ke Di(邸克), Jia-Jia Du(杜佳佳), and Jian-Gong Hu(胡建功)
Chin. Phys. B, 2020, 29 (**12**): 123701. DOI: 10.1088/1674-1056/aba9c9

Movable precision gravimeters based on cold atom interferometry

Jiong-Yang Zhang(张炯阳), Le-Le Chen(陈乐乐), Yuan Cheng(程源), Qin Luo(罗覃), Yu-Biao Shu(舒玉彪), Xiao-Chun Duan(段小春), Min-Kang Zhou(周敏康), Zhong-Kun Hu(胡忠坤)
Chin. Phys. B, 2020, 29 (**9**): 093702. DOI: 10.1088/1674-1056/aba9bc

Comparison of the sensitivities for atom interferometers in two different operation methods

Xiao-Chun Duan(段小春), De-Kai Mao(毛德凯), Xiao-Bing Deng(邓小兵), Min-Kang Zhou(周敏康), Cheng-Gang Shao(邵成刚), Zhu Zhu(祝竺), Zhong-Kun Hu(胡忠坤)
Chin. Phys. B, 2018, 27 (**1**): 013701. DOI: 10.1088/1674-1056/27/1/013701

Common-mode noise rejection using fringe-locking method in WEP test by simultaneous dual-species atom interferometers

Xiao-Bing Deng(邓小兵), Xiao-Chun Duan(段小春), De-Kai Mao(毛德凯), Min-Kang Zhou(周敏康), Cheng-Gang Shao(邵成刚), Zhong-Kun Hu(胡忠坤)
Chin. Phys. B, 2017, 26 (**4**): 043702. DOI: 10.1088/1674-1056/26/4/043702

Direct loading of atoms from a macroscopic quadrupole magnetic trap into a microchip trap

Jun Cheng(程俊), Jing-fang Zhang(张敬芳), Xin-ping Xu(许忻平), Hai-chao Zhang(张海潮), Yu-zhu Wang(王育竹)
Chin. Phys. B, 2017, 26 (**3**): 033701. DOI: 10.1088/1674-1056/26/3/033701

Measuring gravitational effect of superintense laser by spin-squeezed Bose–Einstein condensates interferometer

Eng Boon Ng[†] and C. H. Raymond Ooi[‡]

Department of Physics, University of Malaya, Kuala Lumpur 50603, *Malaysia*

(Received 3 August 2021; revised manuscript received 1 December 2021; accepted manuscript online 11 December 2021)

We consider an extremely intense laser, enclosed by an atom interferometer. The gravitational potential generated from the high-intensity laser is solved from the Einstein field equation under the Newtonian limit. We compute the strength of the gravitational force and study the feasibility of measuring the force by the atom interferometer. The intense laser field from the laser pulse can induce a phase change in the interferometer with Bose–Einstein condensates. We push up the sensitivity limit of the interferometer with Bose–Einstein condensates by spin-squeezing effect and determine the sensitivity gap for measuring the gravitational effect from intense laser by atom interferometer.

Keywords: intense laser field, atom interferometer, Bose–Einstein condensates, spin-squeezing

PACS: 37.25.+k, 67.85.–d **DOI:** 10.1088/1674-1056/ac4231

1. Introduction

Atom interferometer has been developing fast by capitalizing on atomic physics advancements, including cooling, trapping, and deflecting ultracold atoms. Different structures of atom interferometer, for example, Mach–Zehnder type and atomic fountain, have been designed and can achieve high precision measurement. Potential applications of atom interferometer[1] include the testing of general relativity,[2] measurement of gravitational constant,[3] measurements on Berry's phase and inertial forces. The most promising method to measure inertial force is an accelerometer[4] developed from atom interferometer. By using the atom interferometer as accelerometer, the typical sensitivity reaches about $10^{-9}g$ while the maximum sensitivity achieved is about $10^{-12}g$.[1] The force induces a small change in the velocity distribution of the atomic distribution, giving rise to a small change in phase. The atom interferometer is sensitive enough to detect the small phase change. The phase sensitivity of the atom interferometer has been improved with the ultimate aim to achieve the Heisenberg limit, $\delta\phi = 1/N$. Currently, the sensitivity is limited to $\delta\phi = 1/\sqrt{N}$, mainly due to the quantum projection noise.

This high sensitivity has made the atom interferometer a potential tool to reveal the gravitational effect from an intense laser. Observable gravitational effect is always generated by bodies of large masses. However, the source of the gravitational field can also come from the electromagnetic field.[5] Laser, composed of varying electromagnetic fields, is another excellent tool to study gravity on a small scale. It has been predicted laser intensity up to 10^{21} W/cm^2 is able to curve the spacetime and produce artificial gravity.[6]

With the technological prowess and efforts put in by scientists, particularly the ELI group, a high-power laser with peak power of more than 10^{15} W has been invented.[7] By packing energy to a very short lifetime, the power of the laser can be boosted up extremely. Petawatt laser is becoming common because of the technique called chirped-pulse amplification (CPA),[8] which breaks the light pulse into components and amplifies them individually before rejoining them back together. Currently, high-power laser system (HPLS) designed by ELI can create extremely intense pulse[9] with intensity reaching 10^{23} W/cm^2. Powerful pulse amplification technique such as optical parametric chirped pulse amplification (OPCPA), an extended version of CPA, has been designed to compress the laser pulse to sub-fs duration.[9] In this method, a pump beam is used to amplify the signal beam in the OPCPA.

For creating a laser with intensity exceeding 10^{23} W/cm^2, plasma compression of laser pulse using backward Raman scattering[10] is suggested. The interactions of three waves, including pump pulse with ω_a, seed pulse with ω_b and plasma wave with $\omega_p = \omega_a - \omega_b$, cause an energy transfer from pump pulse to seed pulse.[11] The seed pulse produced after CPA and OPCPA can be amplified to femtosecond pulse by using backward Raman scattering. By using this three-step pulse amplification method, better known as cascaded conversion compression,[12] an ambitious but realistic plan to create the exawatt laser[13,14] is now possible. Thus, a laser with an intensity of 10^{25} W/cm^2 is likely to be achieved within the next few years.

Inspired by the idea of high-intensity laser, we aim to study the gravitational effect of high-intensity laser[6,15–17] with the help of an atom interferometer in our paper. The grav-

[†]Corresponding author. E-mail: engboon@live.com.my
[‡]Corresponding author. E-mail: rooi@um.edu.my

© 2022 Chinese Physical Society and IOP Publishing Ltd

itational properties of laser have been explored by.[18–20] The weak gravitational field produced by the laser can be modelled in the framework of linearized gravity. To detect it, we design an atomic interferometer scheme loaded with Bose–Einstein condensate (BEC). To further enhance the sensitivity, tripod scheme is applied to the BEC to produce spin squeezing effect.

2. Gravitational potential

We first compute the gravitational potential from the intense laser. With considering a high-intensity laser beam with radius, $r_{\rm l}$, traveling along the z-axis, its electric and magnetic fields oscillating along the x and y directions, respectively, can be written as

$$\begin{aligned}\boldsymbol{E} &= E_0 \exp\left(-\frac{1}{2}(r/r_{\rm l})^2\right)\exp\left(-\left(\frac{t-z/c}{\tau}\right)^2\right)\sin(k_{\rm l}z-\omega_{\rm l}t)\hat{e}_x,\\ \boldsymbol{B} &= \frac{E_0}{c}\exp\left(-\frac{1}{2}(r/r_{\rm l})^2\right)\exp\left(-\left(\frac{t-z/c}{\tau}\right)^2\right)\sin(k_{\rm l}z-\omega_{\rm l}t)\hat{e}_y,\end{aligned} \tag{1}$$

where $k_{\rm l}=\omega_{\rm l}/c$. The beam we considered is a Gaussian beam, $\exp(-\frac{1}{2}(r/r_{\rm l})^2)$, that ensures the intensity drops rapidly from the centre of the pulse. Our laser beam is modelled as pulses by $\exp(-(\frac{t-z/c}{\tau})^2)$, where τ is the pulse duration. The energy density carried by the electromagnetic field, which acts as the source of gravity, is given by

$$u=\frac{\varepsilon_0}{2}\boldsymbol{E}^2+\frac{1}{2\mu_0}\boldsymbol{B}^2. \tag{2}$$

Here, ε_0 and μ_0 are the permittivity and permeability of free space, respectively. Equation (1) describes the electromagnetic field of linearly polarized laser pulse. As a consequence, the energy density varies sinusoidally as well as dependent on the (Gaussian) envelope of the laser pulse. This is different from the case of circular polarization, where the energy density is constant determined only by the envelope of the laser pulse.[19]

The laser pulse perturbs the flat Minkowski spacetime metric, $\eta_{\mu\nu}=\mathrm{diag}(-1,1,1,1)$, and generates a weak gravitational field, $h_{\mu\nu}\ll 1$, to give a total field of

$$g_{\mu\nu}=\eta_{\mu\nu}+h_{\mu\nu}. \tag{3}$$

By linearizing the Einstein field equation, the small perturbation is governed by[19,20]

$$\left(\nabla^2-\frac{1}{c^2}\frac{\partial^2}{\partial t^2}\right)h_{\mu\nu}=-\frac{16\pi G}{c^4}\left(T_{\mu\nu}-\frac{1}{2}\eta_{\mu\nu}T_{\alpha\beta}\eta^{\alpha\beta}\right), \tag{4}$$

where $T_{\mu\nu}$ is the electromagnetic field tensor that describes the energy flux of μ component passing through the surface in the ν direction. Equation (4) is obtained after imposing Lorentz gauge condition, $\partial^\mu(h_{\mu\nu}-\frac{1}{2}\eta_{\mu\nu}h_{\alpha\beta}\eta^{\alpha\beta})=0$, which requires the energy and momentum to be conserved, $\partial^\mu T_{\mu\nu}=0$.[19] In our case, the laser beam travels along the z-direction, so the non-zero terms are T_{00}, T_{03}, T_{30}, and T_{33}, where $T_{00}=T_{33}=-T_{03}=-T_{30}=u$. Here, we only consider the laser beam contribution to $h_{\mu\nu}$ and ignore the gravitational effect from emitter or receiver.[19] Consequently, four differential equations corresponding to h_{00}, h_{03}, h_{30}, and h_{33} can be obtained from Eq. (4). The solutions of these four equations determine how the new gravitational field changes the trajectories of test particles.

The trajectory of a test particle in the gravitational field is governed by the geodesic equation[19]

$$\frac{\partial^2 x^\mu}{\partial t^2}=-\Gamma^\mu_{\rho\sigma}\frac{\partial x^\rho}{\partial t}\frac{\partial x^\sigma}{\partial t}, \tag{5}$$

where $\Gamma^\mu_{\rho\sigma}$ is the Christoffel symbols. Since the motion of the test particle is slow compared to the speed of light, the term with Γ^μ_{00} is the only significant term in Eq. (5). Moreover, if we consider a two-dimensional test particle by limiting the motion of the test particle in the x^3-direction, then Eq. (5) can be further reduced to

$$\frac{\partial^2 x^\mu}{\partial t^2}=-\frac{c^2}{2}\frac{\partial h_{00}}{\partial x^\mu} \tag{6}$$

with $\mu=1,2$ only. Any deflection of the particle due to the gravity in the xy-plane is determined by Eq. (5). From Eq. (6), we can see that only h_{00} is involved in the motion of the particle, so we ignore the other perturbation terms in Eq. (4). As a consequence, we achieve the Newtonian limit[21] where the metric perturbation is determined solely by h_{00}. From Eq. (4), the oscillating perturbation on the flat spacetime metric satisfies a wave equation

$$\left(\nabla^2-\frac{1}{c^2}\frac{\partial^2}{\partial t^2}\right)h_{00}=-\frac{16\pi G}{c^4}u. \tag{7}$$

To study the effect of gravity, the laser pulse is modelled as a cylindrical beam propagating along the z-direction with the laser axis located at (x_0,y_0,z) (see Fig. 1 below). By defining $\boldsymbol{R}_1$ as BEC interferometer's coordinate and $\boldsymbol{R}_2$ as the laser beam's coordinate, the gravitational potential, V_g generated from metric perturbation by the laser beam can be obtained from the solution of Eq. (7). Using the fact that force is a negative gradient of potential, we can deduce that $V_g=-\frac{mc^2}{2}h_{00}$[21,22] from Eq. (6). Using the Green's function approach,[23] we solve Eq. (7) and obtain

$$V_g(\boldsymbol{R}_1,t) = -\frac{2mG\varepsilon_0 E_0^2}{c^2}\iiint \exp\left(-2\left(\frac{t-\dfrac{|\boldsymbol{R}_1-\boldsymbol{R}_2|}{c}-z/c}{\tau}\right)^2\right)\mathrm{e}^{-(r/r_1)^2}\sin^2\left[k_1 z-\omega_1\left(t-\frac{|\boldsymbol{R}_1-\boldsymbol{R}_2|}{c}\right)\right]\frac{1}{|\boldsymbol{R}_1-\boldsymbol{R}_2|}\mathrm{d}R_2^3, \quad (8)$$

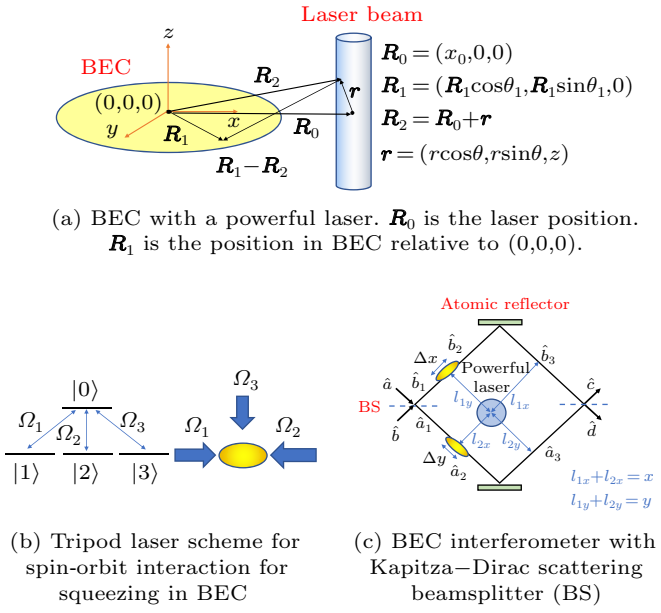
where $t-|\boldsymbol{R}_1-\boldsymbol{R}_2|/c$ is known as retarded time that takes into account the time needed by the gravitational field to travel from its source at $\boldsymbol{R}_2$ to a point at $\boldsymbol{R}_1$. Note that $(1/2)\varepsilon_0 E_0^2 = u_0$ is the peak energy density of the laser. Equation (8) has a similar form as the metric perturbation equation due to the linearly-polarized laser pulse derived in Ref. [19]

From Eq. (8), it is evident that each unit energy along the laser beam at $\boldsymbol{R}_2$ contributes to the gravitational potential at $\boldsymbol{R}_1$. Thus, an integration of Eq. (8) over the total volume of the laser beam is required to compute the gravitational potential. In the cylindrical coordinate, the potential takes the form of

$$V_g(\boldsymbol{R}_1,t) = \frac{mG\varepsilon_0 E_0^2}{c^2}\iiint \exp\left(-2\left(\frac{t-\dfrac{|\boldsymbol{R}_1-\boldsymbol{R}_2|}{c}-z/c}{\tau}\right)^2\right)\mathrm{e}^{-(r/r_1)^2}\left[\cos(2\omega_1 t)\frac{\cos(2k_1 z+2k_1|\boldsymbol{R}_1-\boldsymbol{R}_2|)}{|\boldsymbol{R}_1-\boldsymbol{R}_2|}\right.$$
$$\left.+\sin(2\omega_1 t)\frac{\sin(2k_1 z+2k_1|\boldsymbol{R}_1-\boldsymbol{R}_2|)}{|\boldsymbol{R}_1-\boldsymbol{R}_2|}-\frac{1}{|\boldsymbol{R}_1-\boldsymbol{R}_2|}\right] r\mathrm{d}r\mathrm{d}\theta\mathrm{d}z. \quad (9)$$

Equation (9) consists of three terms. The first two terms describe the fast oscillating gravitational waves generated by the laser beam. These first two terms average to zero for a time scale much greater than the period of the waves due to the rapid oscillating terms, $\sin(2\omega_1 t)$ and $\cos(2\omega_1 t)$. Hence, we focus on the effect of the last term that varies inversely over space. The numerical plots of potential based on Eq. (9) and the local force in the x-direction, F_g computed from the gradient of the gravitational potential, $\boldsymbol{F} = -\nabla V_g$,[24] are provided in Appendix A. In general, the potential is time-dependent because of the envelope function we set for a pulse, the potential does not vary much within τ (see Appendix A). For time larger than τ, the potential becomes insignificant due to $\exp(-2(\frac{t-\frac{|\boldsymbol{R}_1-\boldsymbol{R}_2|}{c}-z/c}{\tau})^2)$ in Eq. (9). For simplicity, we first assume the potential experienced by the BEC interferometer is constant, similar to potential generated from uniform beam.[18] The effect of pulse characteristics, governed by pulse duration and repetition rate, on the gravitational force strength will be discussed below.

The laser parameters we considered produce high power in the petawatt range. The pulse of the laser with pulse energy of 2 kJ is compressed to 1 ps to produce the high-power laser pulse.[9,25,26] The beam size is $r_1 = 10$ μm so the intensity of the laser is about 10^{21} W/cm^2. Besides, we also consider the exawatt laser with power in the range of 10^{18} W by increasing the pulse energy to 2 MJ. The intensity we considered is 10^{24} W/cm^2. The exawatt laser and zettawatt laser are possible to realize according to Ref. [13] and the exawatt laser is currently under construction. From the laser parameters, the average force per atom can be estimated to give $F_g \approx 10^{-42}$ N or acceleration, $\delta g = 10^{-19} g$ for petawatt laser, and $F_g \approx 10^{-39}$ N or $\delta g = 10^{-16} g$ for exawatt laser. For petawatt laser, the strength of acceleration produced by the linearly polarized Gaussian pulse is consistent with the circularly-polarized laser pulse in Ref. [19].



(a) BEC with a powerful laser. $\boldsymbol{R}_0$ is the laser position. $\boldsymbol{R}_1$ is the position in BEC relative to (0,0,0).

(b) Tripod laser scheme for spin-orbit interaction for squeezing in BEC

(c) BEC interferometer with Kapitza–Dirac scattering beamsplitter (BS)

Fig. 1. (a) Vector coordinates in BEC and a powerful laser. (b) Tripod scheme acting on the BEC creating spin-squeezing effect is created at the beginning of the path, Δx and Δy. Ω_i is the Rabi frequency of the laser to couple the internal state of the BEC. (c) Schematic of a spin-squeezed BEC interferometer. The laser beam is placed near the lower path of the interferometer, $x_0 = 0.5$ mm. Optical standing wave acts as beam splitter (blue dotted line) and mirror (red line) for the BEC. Circle at center represents the gravitational source at (x_0, y_0), is allowed to vary along the arm length of the interferometer, $l_{1x}+l_{2x}$. The gravitational force is perpendicular to the arm, inducing a phase shift in the BEC and affecting the interference fringes at the output. The effect of deflection by the gravitational force is less important than the phases induced on the arms. In practice any deflection can be corrected to avoid a loss of contrast.

3. Atomic interferometer

We are concerned about the strength of the laser parameters to produce gravitational effect, and the possibility to measure the small perturbation. From previous studies,[19] the de-

flection of test particles by gravity is, in general, too small to be measured. Instead, the phase shift of atoms has been proposed to study the gravity generated from the high-power laser. The interferometric detection method is usually employed to detect the slight phase shift. To produce a measurable phase shift, a long optical traveling path is necessary.[16,27] Besides, by using the collective oscillation, BEC has been suggested to be used as a sensor to detect gravitational wave[28] and oscillating gravitational field.[29] The main advantages of using BEC as a medium in the interferometer are also obvious over the typical ultracold atom. Large coherence length of BEC and narrow velocity distribution give high fringe contrast, better beam-splitting efficiency and large momentum beam-splitting.[4,30,31] BEC in the squeezed state offers a great improvement in signal to noise ratio.[4]

In our case, we demonstrate a BEC interferometer scheme, as illustrated in Fig. 1, to detect the acceleration caused by the intense laser. The optical standing wave, acting as beam splitter or mirror in the interferometer, can manipulate the de-Broglie waves of BEC with different momentum.[32,33] Initially, BEC is split into two groups, approximately 25% of condensate, by letting the BEC passes through the optical standing wave. Diffraction of the atomic wave by the standing wave into momentum states with $\pm\hbar k_{\rm eff}$ occurs, which is known as Kapitza–Dirac scattering.[32,33] These two groups of atoms travel to two different paths in the interferometer and undergo free evolution while experiencing the force from the intense laser as well as the geometric phase. Note that the intense laser is entirely enclosed by the interferometer's arms and is not placed exactly at the center of the interferometer. At time T, optical standing wave is applied to reflect the BEC. Now, the optical standing wave is considered as two waves traveling opposite to each other. $N_{\rm B}$ photons are transferred between the two traveling waves, giving rise to a total exchange of momentum, $2N_{\rm B}\hbar k_{\rm eff}$ from photons to the bosons. This is known as Bragg scattering.[32,33] Finally, after traveling for $2T$, these two groups of BEC are recombined coherently. Spatial fringes are formed, revealing the phase difference caused by the acceleration.

In contrast to the conventional Mach–Zehnder interferometer, tripod scheme,[34–37] which has been used in creating spin–orbit coupling effect in ultracold atoms, is applied at the beginning of each path (Δx and Δy in Fig. 1) to generate a non-Abelian gauge field that affects the spin behavior. Three lasers in a particular arrangement couple the degenerate internal states of ^{87}Rb, including $|1\rangle$, $|2\rangle$, and $|3\rangle$ together, to produce the pseudospin by Rabi frequencies, $\Omega_1 = |\Omega_1|e^{-iS_1}$, $\Omega_2 = |\Omega_2|e^{-iS_2}$ and $\Omega_3 = |\Omega_3|e^{-iS_3}$. After solving the Hamiltonian of the tripod scheme, the dressed states[34,35,37] are given as

$$\begin{aligned}|D_1\rangle &= \sin\phi_{\rm I} e^{-iS_{13}}|1\rangle - \cos\phi_{\rm I} e^{-iS_{23}}|2\rangle,\\ |D_2\rangle &= \cos\theta_{\rm I}\cos\phi_{\rm I} e^{-iS_{13}}|1\rangle + \cos\theta_{\rm I}\sin\phi_{\rm I} e^{-iS_{23}}|2\rangle\\ &\quad - \sin\theta_{\rm I}|3\rangle,\end{aligned} \tag{10}$$

where $\theta_{\rm I}$ and $\phi_{\rm I}$ govern the relative intensities between lasers and $S_{ij} = S_1 - S_j$. We define the two dressed states, $|D_1\rangle$ and $|D_2\rangle$, as $|\uparrow\rangle$ and $|\downarrow\rangle$ respectively. Before splitting by Kapitza–Dirac scattering, the BEC is prepared in the dressed state of $|\downarrow\rangle = -|3\rangle$ for $\theta_{\rm I} = (\pi/2)$.

The phase change of the BEC induced by the gauge field is $\phi_{\rm L} = -(1/\hbar)\int_{r_{\rm i}}^{r_{\rm f}} \boldsymbol{A}(\boldsymbol{r})\,{\rm d}r$,[34] where the vector potential is defined as $\boldsymbol{A}(\boldsymbol{r}) = i\hbar\langle D|\nabla D\rangle$. Manipulating the intensities of the three lasers,[36] we obtain the vector potential as $\boldsymbol{A}(\boldsymbol{r}) = m\lambda_{\rm R}(\sigma_y, -\sigma_x)$, a same form as Rashba spin–orbit interaction,[38,39] where $\lambda_{\rm R} = (\hbar k_{\rm R})/m$ is the spin–orbit coupling strength and $\hbar k_{\rm R}$ is recoil momentum from the lasers. The phase change due to the vector potential is different depending on the path taken by BEC, which is known as the Aharonov–Bohm effect.[37] From $e^{i\phi_{\rm L}}$, the gauge field rotates the spin direction[37] of lower path about x-axis by

$$e^{ik_{\rm R}\Delta y\sigma_x} = \begin{pmatrix}\cos(k_{\rm R}\Delta y) & i\sin(k_{\rm R}\Delta y)\\ i\sin(k_{\rm R}\Delta y) & \cos(k_{\rm R}\Delta y)\end{pmatrix}, \tag{11}$$

and upper path about y-axis by

$$e^{-ik_{\rm R}\Delta x\sigma_y} = \begin{pmatrix}\cos(k_{\rm R}\Delta x) & -\sin(k_{\rm R}\Delta x)\\ \sin(k_{\rm R}\Delta x) & \cos(k_{\rm R}\Delta x)\end{pmatrix}. \tag{12}$$

Δx and Δy are the length scales where lasers have the strongest intensity[34] to couple the internal states. As mentioned in Ref. [34], the velocity of BEC is generally faster than the recoil velocity, $\lambda_{\rm R} = 0.5$ cm/s. Hence, the non-Abelian gauge field only affects the internal state of the BEC without having any effect on the center of mass dynamics.

Now, we determine the effect of the gauge field on the output of the interferometer. Let $a^\dagger$ and $b^\dagger$ be the annihilation operators for boson at the two inputs, and the output boson number operators[40] (see Appendix B) are

$$\begin{aligned}\hat{c}^\dagger\hat{c} &= \frac{1}{2}[1+\sin^2(k_{\rm R}\Delta x)\sin\phi - \cos^2(k_{\rm R}\Delta x)\cos\phi]\hat{a}^\dagger\hat{a}|\downarrow\rangle\langle\downarrow| + \frac{1}{2}[\sin^2(k_{\rm R}\Delta x)\cos\phi + \cos^2(k_{\rm R}\Delta x)\sin\phi](\hat{a}^\dagger\hat{b}+\hat{b}^\dagger\hat{a})|\downarrow\rangle\langle\downarrow|\\ &\quad + \frac{1}{2}[1-\sin^2(k_{\rm R}\Delta x)\sin\phi + \cos^2(k_{\rm R}\Delta x)\cos\phi]\hat{b}^\dagger\hat{b}|\downarrow\rangle\langle\downarrow|,\end{aligned} \tag{13}$$

$$\begin{aligned}\hat{d}^\dagger\hat{d} &= \frac{1}{2}[1-\sin^2(k_{\rm R}\Delta x)\sin\phi + \cos^2(k_{\rm R}\Delta x)\cos\phi]\hat{a}^\dagger\hat{a}|\downarrow\rangle\langle\downarrow| + \frac{1}{2}[-\sin^2(k_{\rm R}\Delta x)\cos\phi - \cos^2(k_{\rm R}\Delta x)\sin\phi](\hat{a}^\dagger\hat{b}+\hat{b}^\dagger\hat{a})|\downarrow\rangle\langle\downarrow|\\ &\quad + \frac{1}{2}[1+\sin^2(k_{\rm R}\Delta x)\sin\phi - \cos^2(k_{\rm R}\Delta x)\cos\phi]\hat{b}^\dagger\hat{b}|\downarrow\rangle\langle\downarrow|.\end{aligned} \tag{14}$$

We now define $\phi = (\mu - \upsilon)$ with $\mu = k_{1x}x + k_{1y}y$ and $\upsilon = k_{2x}x + k_{2y}y$ for the phase shift measured by the interferometer. It can be easily shown that $\langle \hat{c}^\dagger \hat{c} + \hat{d}^\dagger \hat{d} \rangle = \langle \hat{a}^\dagger \hat{a} + \hat{b}^\dagger \hat{b} \rangle$ for particle number conservation. To determine the phase difference, we compute the difference in mean boson number, $\hat{M} = \hat{d}^\dagger \hat{d} - \hat{c}^\dagger \hat{c}$ between the two outputs,[40] yielding

$$\begin{aligned}\hat{M} = {} & [-\sin^2(k_{\mathrm{R}}\Delta x)\sin\phi + \cos^2(k_{\mathrm{R}}\Delta x)\cos\phi]\hat{a}^\dagger\hat{a}\,|\downarrow\rangle\langle\downarrow| + [-\sin^2(k_{\mathrm{R}}\Delta x)\cos\phi - \cos^2(k_{\mathrm{R}}\Delta x)\sin\phi](\hat{a}^\dagger\hat{b} + \hat{b}^\dagger\hat{a})\,|\downarrow\rangle\langle\downarrow| \\ & + [\sin^2(k_{\mathrm{R}}\Delta x)\sin\phi - \cos^2(k_{\mathrm{R}}\Delta x)\cos\phi]\hat{b}^\dagger\hat{b}\,|\downarrow\rangle\langle\downarrow|. \end{aligned} \tag{15}$$

The tripod scheme does contribute to the output number difference. For one input interferometer, $\langle \hat{a}^\dagger \hat{a} \rangle = N$ and $\langle \hat{b}^\dagger \hat{b} \rangle = 0$, the phase shift generated by the tripod scheme results in $\langle M \rangle = N\cos^2(k_{\mathrm{R}}\Delta x)$ when $\phi = 0$. Since k_{R} and Δx are the values set in experiment, $\cos^2(k_{\mathrm{R}}\Delta x)$ is merely a constant that can be computed and should not cause any difficulty in measuring the unknown ϕ. To see how the tripod scheme affects the phase sensitivity, we compute the phase sensitivity equation by

$$\Delta\phi = \frac{\Delta M}{\left|\dfrac{\partial\langle M\rangle}{\partial\phi}\right|}, \tag{16}$$

where $(\Delta M)^2 = \langle M^2\rangle - \langle M\rangle^2$. From Eq. (16), the phase measurement is limited by the error of counting the difference in boson number between the two outputs.

By launching BEC at one input, the coherent wavefunction can be written as $|\psi\rangle_{\mathrm{A}}|\psi\rangle_{\mathrm{B}} = |\alpha,\downarrow\rangle|0,\downarrow\rangle$, where $|\alpha|^2 = N$. Using the initial wavefunction together with Eq. (16), we reach the standard quantum limit (SQL) for phase measurement, $\Delta\phi = 1/\sqrt{N}$ (see Appendix C). SQL is the ideal sensitivity of phase measurement by usual interferometer with one input[40] but not maximum sensitivity. To measure the force from intense laser, the phase sensitivity should reach the Heisenberg limit, $\Delta\phi = 1/N$. An interferometer with a large number of bosons, at least 10^6, is expected to overcome the shot-noise limit.[30] However, using high N causes the 2-body interaction to be significant, giving rise to the mean-field shift. For high N, a particular correction on the final result is required to remove the mean-field effect, as shown in Ref. [41]. Besides, studies of high precision interferometers by using two input ports with incident particles including photons in the squeezed state,[42] spin-$(1/2)$ particles,[43] and spin-squeezed BEC,[31] have shown to be able to achieve Heisenberg limit.

For our interferometer scheme, to enhance the phase sensitivity, the spin properties under the influence of non-Abelian gauge field has to be considered in the phase sensitivity calculation. Previous studies show that the spin–orbit coupling effect[44–46] can lead to spin squeezing, providing an important boost in the phase sensitivity to approach the Heisenberg limit. By reducing the quantum fluctuation of a spin operator in one direction at the expense of the fluctuations in the other two spin operators, precision in the measurement of phase[47] can be significantly enhanced by

$$\Delta\phi = \frac{\xi_i}{\sqrt{N}}, \tag{17}$$

where ξ_i is the spin-squeezing parameter. In general, the spin squeezing parameter[44–46,48] is defined as

$$\xi_i^2 = \frac{4\min(\Delta S_{n_\perp}^2)}{N}, \tag{18}$$

where $(\Delta S_{n_\perp})^2 = \langle S_{n_\perp}^2\rangle - \langle S_{n_\perp}\rangle^2$. $\boldsymbol{S}_{n_\perp}$ is the spin along the direction perpendicular to spin vector $\boldsymbol{S}$, where $|\boldsymbol{S}| = \sqrt{\langle S_x\rangle^2 + \langle S_y\rangle^2 + \langle S_z\rangle^2}$ is the mean spin value. Here, the spin components are defined as $S_i = (1/2)\sigma_i$ with σ_i denoting the Pauli matrix.

Starting with the initial wavefunction, $|\psi\rangle_{\mathrm{A}}|\psi\rangle_{\mathrm{B}} = |\alpha,\downarrow\rangle|0,\downarrow\rangle$, the spin state is also known as a coherent spin state[44–46,48] with all the particles staying at $|\downarrow\rangle$. The mean spin direction is along $-z$-axis and hence $\boldsymbol{S}_{n_\perp}$ is any spin vector in the xy-plane, $|\boldsymbol{S}_{n_\perp}| = \sqrt{\langle S_x\rangle^2 + \langle S_y\rangle^2}$. It is easy to show that $\langle S_x^2\rangle = \langle S_y^2\rangle = N/4$ and $\langle S_x\rangle = \langle S_y\rangle = 0$. Immediately, we can see that $\xi_x^2 = \xi_y^2 = 1$ and phase sensitivity reduces to SQL. Spin squeezing occurs when the fluctuation in $S_{n_\perp}$, characterized by $\Delta S_{n_\perp}^2$, is smaller than $N/4$. In our case, introducing the non-Abelian gauge field to spinful bosons induces SU(2) rotation, closely related to spin squeezing.[48] After a small angle spin rotation acting on $|\downarrow\rangle$ by Eqs. (11) and (12), the mean spin direction is still along z-axis, $|\boldsymbol{S}| \approx \langle S_z\rangle$, but now either $\langle S_x\rangle$ or $\langle S_y\rangle$ is non-zero depending on the rotation axis, so $\Delta S_{n_\perp}^2 < N/4$. We compute the spin squeezing parameter in the x-direction for upper path

$$\xi_x^2 = \cos^2(2k_{\mathrm{R}}\Delta x), \tag{19}$$

and y-direction for lower path

$$\xi_y^2 = \cos^2(2k_{\mathrm{R}}\Delta y), \tag{20}$$

after spin rotation. Spin squeezing that can reduce the quantum phase fluctuation by half occurs if $2k_{\mathrm{R}}\Delta x = (\pi/3) + 2n\pi$. Hence, ξ_i can help improve the sensitivity of phase measurement by one order.

After getting the phase sensitivity of the interferometer, we can proceed to discuss the feasibility of measuring the gravitational effect from the intense laser. To determine the gravitational effect, the point, (x_0, y_0) in Fig. 1 is replaced with intense laser. The gravitational potential from the intense laser

is modelled by Eq. (9). For simplicity, we assume the force is always perpendicular to the interferometer arms acting towards the intense laser. The gravitational force of the intense laser imparts an acceleration, δg on the BEC with total mass of $m_{\rm B} = Nm$ and leads to a small change in phase of BEC, ϕ. The path traveled by BEC under the influence of gravity can be treated as a perturbation on Lagrangian dynamics.[49] The phase change of BEC is $e^{i(L/\hbar)\Delta t}$, where $L = L_0 + \lambda L_1$ is total Lagrangian, L_0 is unperturbed Lagrangian and λL_1 is perturbation Lagrangian with order λ. Without gravity, $L = L_0 = (m_{\rm B}\dot{x}^2)/2$, BEC travels along straight line with its phase, $e^{i(L/\hbar)\Delta t}$ reducing to $e^{i(kx-\omega t)}$.[49] Under the influence of gravity, the BEC is attracted toward the laser, and hence the path is deflected slightly. For simplicity, we first assume the acceleration is constant at g with direction pointing towards a reference point at (x_0, y_0) where potential energy is zero. The Lagrangian equations with gravity as the perturbation for each arm are given as

$$L_{1x}(\dot{y}, y) = L_{2x}(\dot{y}, y) = \frac{m_{\rm B}\dot{y}^2}{2} - m_{\rm B} g\,|y - y_0|\,,$$
$$L_{2y}(\dot{x}, x) = L_{1y}(\dot{x}, x) = \frac{m_{\rm B}\dot{x}^2}{2} - m_{\rm B} g\,|x - x_0|\,. \quad (21)$$

The point, (x_0, y_0), is not placed exactly at the center so that for upper path and lower path, the gravitational potentials in the x-direction are $m_{\rm B} g l_{1x}$ and $m_{\rm B} g l_{2x}$ respectively. The difference in gravitational potential that contributes to the phase shift is given as $m_{\rm B} g(l_{2x} - l_{1x})$. Thus, we can compute the phase shift between the two paths by integrating the perturbation Lagrangian along the unperturbed path,[49] $\phi = (1/\hbar)\oint \lambda L_1\,{\rm d}t$ to obtain

$$\phi = \frac{m_{\rm B} g}{\hbar}(l_{2x} - l_{1x})T. \quad (22)$$

Note that the gravitational effect in the y-direction cancels out each other due to our interferometer scheme.

Using Eq. (22), we can estimate the smallest measurable acceleration by the interferometer from

$$\delta g = \frac{\hbar\cos(2k_{\rm R}\Delta x)}{m_{\rm B} g(l_{2x} - l_{1x})T\sqrt{N}}\, g. \quad (23)$$

Assuming the BEC of $N = 10^5$ travelling at 0.3 m/s with the interferometer arm's length equals to 3 mm, T is about 10ms. By using Eqs. (17) and (23), the smallest change in acceleration that can be detected is estimated at $\delta g = 10^{-15} g$. The gravitational effect from the petawatt laser is too small to be measured by the interferometer. If exawatt laser can be built, the acceleration is just one order less than the sensitivity of the BEC interferometer. Note that T cannot be set too high as it will affect the high contrast due to BEC losing its coherence. However, decoherence caused by interaction can be eliminated[50] by tuning the scattering length to almost zero using Feshbach resonance. Therefore, coherence time of BEC reaching 10 s is possible in experiment.[51]

Equation (23) is based on the assumption that the gravitational acceleration due to the laser pulse is present for the whole duration as the BEC travels through the arms of the interferometer. This is necessary for the phase difference along the two paths in the BEC interferometer to accumulate enough so that the gravitational effect can be emerged. However, the effective interaction time for the gravitational potential of the laser pulse to act on the BEC interferometer is extremely short, $t_{\rm eff} = \tau f_{\rm rep} T$, where $f_{\rm rep}$ is the repetition rate. So, the actual average acceleration, $\delta\bar{g} = \delta g \times (t_{\rm eff}/T)$ can be computed and shown to be in the order of $10^{-23} g$ for exawatt laser with $f_{\rm rep} = 10^6$ Hz. The average acceleration is just too small even when the exawatt laser is measured by the most precise phase measurement device. The power of laser has been improved a lot recently; however, the low repetition rate is one of the main limitations to measure the gravitational effect.

To achieve a high repetition rate,[26] a source with high average power is required. One of the possible methods is the diode laser pumping technology. ELI lasers, which are diode-pumped, can produce a laser pulse of 0.1 J energy at repetition rate of kHz. For pulse energy of 1 kJ, the highest rate achieved by HPLS is 1 pulse per minute. Instead of searching for a higher average power source, an alternative is to generate multiple gravitational effects by just a single pulse. Waveguide[52] or ring cavity[53] can be applied to engineer a looping trajectory so that a pulse can repeatedly generate gravitational effect on the atom interferometer. The time for the laser pulse to complete a loop or an oscillation corresponds to the pulse period or the repetition rate of a laser. Recently, an idea of letting short laser pulse oscillating with a high frequency in a cavity is proposed[54] to amplify the power of laser pulse. The power amplification factor up to 10^3 is possible. However, the powerful laser, for example ELI laser, still cannot be used as pump laser in their system because the high power laser pulse can damage the cavity and has a low repetition rate. Nevertheless, the effort of realising the oscillation of high power laser pulse in the cavity brings the hope of creating larger gravitational effect by a single laser pulse.

4. Conclusion

We have derived the gravitational potential of the high-intensity laser and designed a spin-squeezed BEC interferometer with improved sensitivity to measure the gravitational effect. The weak attractive force from the gravitational potential can cause a small spatial displacement of the BEC in the interferometer. We determine the laser parameters, which may produce measurable results. The laser parameters we considered are realistic and aligned with the current intense laser

development. Even though the gravitational force created by the intense laser is extremely small, it induces variations in the phase of the BEC interferometer. We derive the sensitivity equation of the BEC interferometer to determine the feasibility of detecting the small phase shift. Conventional interferometer is limited by SQL. While other parameters, for example, the number of particles, are subjected to physical limitations, and spin squeezing is the most promising method to improve phase sensitivity below SQL. We create the spin squeezing effect in the BEC interferometer by introducing the non-Abelian gauge field using tripod scheme. Even though the BEC interferometer's sensitivity and the power of intense laser have been greatly enhanced, the gravitational effect from intense laser remains too small to be measured. The repetition rate and pulse duration determine the effective time of gravitational potential acting on the BEC interferometer. Since these two parameters for the intense laser are extremely low, the phase accumulation in the BEC interferometer is not enough to produce measurable results. An improved design that significantly increases the effective interaction time between the high energy laser pulses and the BEC is needed to achieve a detectable phase shift in the interferometer.

Acknowledgment

R.O. thanks the support by Ministry of Higher Education Malaysia under Long-Term Research Grant Scheme, LRGS/1/2020/UM/01/5/1.

Appendix A

In this section, we perform the numerical calculation for petawatt laser using the laser parameters mentioned above. The (non-oscillating) last term of Eq. (9) and force at different times are plotted. From Fig. A1, the gravitational potential has a slope going down towards the laser beam. When getting closer to the laser beam, the potential should vary as $\ln(r)$,[18] where r is defined as the distance to the laser beam. Thus, the force exhibits a $1/r$ dependence, which is attractive towards the laser beam and is stronger when nearer to the laser beam. We can see the pulse is modulated by $\exp(-2(\frac{t-\frac{|\boldsymbol{R}_1-\boldsymbol{R}_2|}{c}-z/c}{\tau}))$. The magnitudes of V_g and F_g are maximum at $t=0$ because the pulse is closest to the BEC interferometer at $z=0$. When t increases, the pulse moves away from $z=0$ by $z=ct$, so the strength drops monotonously. However, as shown in Fig. A2, the magnitudes of V_g and F_g do not vary much for time range within τ. We assume the force strength is constant at its maximum value in above calculations.

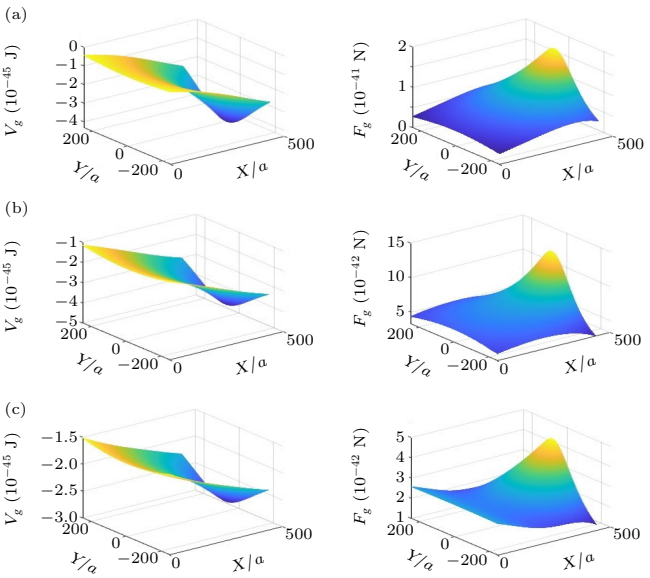


Fig. A1. Gravitational potential (left) from Eq. (9) and force (right) at time, (a) $t=0$, (b) $t=0.5$ ps and (c) $t=\tau=1$ ps. We use the parameters: pulse of 2 kJ energy, $\tau=10^{-12}$ s, and beam radius of $r_1=10$ μm. The distance to the beamline is set at $x_0=0.5$ mm and $z_0=1$ mm. Since the radial dependence of Eq. (9) has a Gaussian profile, we cutoff the integration over r at $3r_1$ for Eq. (9). Note that spatial dimensions are reduced by $a=9.12\times10^{-7}$ m.

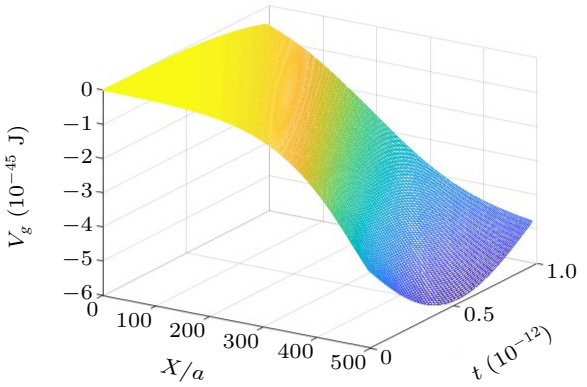


Fig. A2. (a) Gravitational potential along $Y=0$ for $t=0$ to $t=\tau$. The laser parameters used are the same as Fig. A1.

Appendix B

In this section, we derive the output number operators based on the input number operators. We label the upper input port as A and the lower input port as B. Assuming both of the inputs are incident with BEC, the coherent wavefunction is $|\psi\rangle_{\rm A}|\psi\rangle_{\rm B}=|\alpha,\downarrow\rangle|\beta,\downarrow\rangle$, whose average boson numbers at each input port are $\langle a^\dagger a\rangle=|\alpha|^2=N_{\rm A}$ and $\langle b^\dagger b\rangle=|\beta|^2=N_{\rm B}$. After the BEC passing through the first beam-splitter, we assume the BEC is separated equally to the two interferometer's paths and its phase is π shifted. So, now the operators after the first beam-splitter transform to

$$\begin{pmatrix}\hat{a}_1\\ \hat{b}_1\end{pmatrix}=\frac{1}{\sqrt{2}}\begin{pmatrix}-1 & \mathrm{i}\\ \mathrm{i} & -1\end{pmatrix}\begin{pmatrix}\hat{a}\\ \hat{b}\end{pmatrix}. \tag{B1}$$

Immediately after the beam splitter, tripod scheme is applied to induce spin squeezing. The phase change due to the tripod

scheme is described by $e^{i\theta_L}$, which is also known as spin rotation as shown in Eqs. (11) and (12) above. The operators now are

$$\begin{pmatrix}\hat{a}_2\\ \hat{b}_2\end{pmatrix}=\begin{pmatrix}e^{i(1/\hbar)m\lambda_R\sigma_x\Delta y} & 0\\ 0 & e^{-i(1/\hbar)m\lambda_R\sigma_y\Delta x}\end{pmatrix}\begin{pmatrix}\hat{a}_1\\ \hat{b}_1\end{pmatrix}. \quad \text{(B2)}$$

Phase accumulation occurs for BEC traveling along the interferometer arm. After traveling for time, $t=2T$, the operators experience a phase change, yielding

$$\begin{pmatrix}\hat{a}_3\\ \hat{b}_3\end{pmatrix}=\begin{pmatrix}ie^{i\upsilon} & 0\\ 0 & ie^{i\mu}\end{pmatrix}\begin{pmatrix}\hat{a}_2\\ \hat{b}_2\end{pmatrix}, \quad \text{(B3)}$$

where $\mu=k_{1x}x+k_{1y}y$ and $\upsilon=k_{2x}x+k_{2y}y$. Note that at $t=T$, the reflection of BEC causes a $\pi/2$ shift in the phase that is included in Eq. (B3). In the end, the final beam splitter transforms the operators to give

$$\begin{pmatrix}\hat{c}\\ \hat{d}\end{pmatrix}=\frac{1}{\sqrt{2}}\begin{pmatrix}-1 & i\\ i & -1\end{pmatrix}\begin{pmatrix}\hat{a}_3\\ \hat{b}_3\end{pmatrix}. \quad \text{(B4)}$$

A simple equation of output operators can be expressed from input operators as

$$\begin{pmatrix}\hat{c}\\ \hat{d}\end{pmatrix}=\frac{1}{2}\begin{pmatrix}ie^{i(1/\hbar)m\lambda_R\sigma_x\Delta y}e^{i\upsilon}-ie^{-i(1/\hbar)m\lambda_R\sigma_y\Delta x}e^{i\mu} & e^{i\frac{1}{\hbar}m\lambda_R\sigma_x\Delta y}e^{i\upsilon}+e^{-i(1/\hbar)m\lambda_R\sigma_y\Delta x}e^{i\mu}\\ e^{i(1/\hbar)m\lambda_R\sigma_x\Delta y}e^{i\upsilon}+e^{-i(1/\hbar)m\lambda_R\sigma_y\Delta x}e^{i\mu} & -ie^{i\frac{1}{\hbar}m\lambda_R\sigma_x\Delta y}e^{i\upsilon}+ie^{-i(1/\hbar)m\lambda_R\sigma_y\Delta x}e^{i\mu}\end{pmatrix}\begin{pmatrix}\hat{a}\\ \hat{b}\end{pmatrix}. \quad \text{(B5)}$$

To obtain Eq. (B5) in the form as Eqs. (13) and (14), we rewrite the terms, $e^{-ik_R\Delta x\sigma_y}$ and $e^{ik_R\Delta y\sigma_x}$, in bra-ket notation to get

$$\begin{aligned}e^{-ik_R\Delta x\sigma_y}&=\cos(k_R\Delta x)\,|\uparrow\rangle\langle\uparrow|-\sin(k_R\Delta x)\,|\uparrow\rangle\langle\downarrow|+\sin(k_R\Delta x)\,|\downarrow\rangle\langle\uparrow|+\cos(k_R\Delta x)\,|\downarrow\rangle\langle\downarrow|,\\ e^{ik_R\Delta y\sigma_x}&=\cos(k_R\Delta y)\,|\uparrow\rangle\langle\uparrow|+i\sin(k_R\Delta y)\,|\uparrow\rangle\langle\downarrow|+i\sin(k_R\Delta y)\,|\downarrow\rangle\langle\uparrow|+\cos(k_R\Delta y)\,|\downarrow\rangle\langle\downarrow|.\end{aligned} \quad \text{(B6)}$$

For simplicity, we assume $\Delta x=\Delta y$ and ignore the terms with $|\uparrow\rangle\langle\uparrow|$ and $|\downarrow\rangle\langle\uparrow|$ in computing Eqs. (13) and (14) since we only consider $|\downarrow\rangle$ in our initial wavefunction.

Appendix C

We show how to get SQL for the interferometer by calculating Eq. (16) explicitly for the case of BEC with mean number of bosons, N, entering one input port. The initial wavefunction is $|\psi\rangle_A|\psi\rangle_B=|\alpha,\downarrow\rangle|0,\downarrow\rangle$. The incident particle is BEC so we use coherent state in the calculation. By using the properties of coherent state, $\hat{a}|\alpha\rangle=\alpha|\alpha\rangle$ and $\langle\hat{a}^\dagger\hat{a}\rangle=|\alpha|^2$, the terms, $\langle\hat{a}^\dagger\hat{b}\rangle$ and $\langle\hat{b}^\dagger\hat{a}\rangle$ can be shown to be zero since $|\psi\rangle_B$ is a vacuum state. Thus, the average difference in boson number computed from Eq. (15) is

$$\langle M\rangle=N[-\sin^2(k_R\Delta x)\sin\phi+\cos^2(k_R\Delta x)\cos\phi]. \quad \text{(C1)}$$

Now, $\langle M\rangle^2$ and $\frac{\partial\langle M\rangle}{\partial\phi}$ can be easily derived from Eq. (C1) to give

$$\langle M\rangle^2=N^2[-\sin^2(k_R\Delta x)\sin\phi+\cos^2(k_R\Delta x)\cos\phi]^2, \quad \text{(C2)}$$

$$\frac{\partial\langle M\rangle}{\partial\phi}=N[-\sin^2(k_R\Delta x)\cos\phi-\cos^2(k_R\Delta x)\sin\phi]. \quad \text{(C3)}$$

Next, to compute the variance, we square the operator, Eq. (15) to get

$$\begin{aligned}\hat{M}^2 &= [-\sin^2(k_R\Delta x)\sin\phi+\cos^2(k_R\Delta x)\cos\phi]^2\hat{X}^2+[-\sin^2(k_R\Delta x)\cos\phi-\cos^2(k_R\Delta x)\sin\phi]^2\hat{Y}^2\\ &\quad+[-\sin^2(k_R\Delta x)\sin\phi+\cos^2(k_R\Delta x)\cos\phi][-\sin^2(k_R\Delta x)\cos\phi-\cos^2(k_R\Delta x)\sin\phi](\hat{X}\hat{Y}+\hat{Y}\hat{X}),\end{aligned} \quad \text{(C4)}$$

where $\hat{X}=\hat{a}^\dagger\hat{a}-\hat{b}^\dagger\hat{b}$ and $\hat{Y}=\hat{a}^\dagger\hat{b}+\hat{b}^\dagger\hat{a}$. Normal ordering can be done on the product of operators by using commutation relation for bosons, $[\hat{a},\hat{a}^\dagger]=1$, to get $\langle X^2\rangle=N^2+N$, $\langle Y^2\rangle=N$, and $\langle XY\rangle=\langle YX\rangle=0$. So, we obtain

$$\langle M^2\rangle=(N^2+N)[-\sin^2(k_R\Delta x)\sin\phi+\cos^2(k_R\Delta x)\cos\phi]^2+N[-\sin^2(k_R\Delta x)\cos\phi-\cos^2(k_R\Delta x)\sin\phi]^2, \quad \text{(C5)}$$

and variance can be computed as

$$(\Delta M)^2=N[-\sin^2(k_R\Delta x)\sin\phi+\cos^2(k_R\Delta x)\cos\phi]^2+N[-\sin^2(k_R\Delta x)\cos\phi-\cos^2(k_R\Delta x)\sin\phi]^2. \quad \text{(C6)}$$

Finally, SQL is reached since the phase sensitivity is proportional to $1/\sqrt{N}$, as shown below:

$$\Delta\phi = \frac{\sqrt{[-\sin^2(k_R\Delta x)\sin\phi+\cos^2(k_R\Delta x)\cos\phi]^2+[-\sin^2(k_R\Delta x)\cos\phi-\cos^2(k_R\Delta x)\sin\phi]^2}}{\sqrt{N}\,|[-\sin^2(k_R\Delta x)\cos\phi-\cos^2(k_R\Delta x)\sin\phi]|}=O\left(\frac{1}{\sqrt{N}}\right). \quad \text{(C7)}$$

References

[1] Wang J 2015 *Chin. Phys. B* **24** 053702
[2] Abbott B P *et al.* 2016 *Phys. Rev. Lett.* **116** 061102
[3] Rosi G, Sorrentino F, Cacciapuoti L, Prevedelli M and Tino G 2014 *Nature* **510** 518
[4] Hardman K S, Everitt P J, McDonald G D, Manju P, Wigley P B, Sooriyabandara M A, Kuhn C C N, Debs J E, Close J D and Robins N P 2016 *Phys. Rev. Lett.* **117** 138501
[5] Bertotti B 1959 *Phys. Rev.* **116** 1331
[6] Ji P, Bai Y and Wang L 2007 *Phys. Rev. D* **75** 024010
[7] Gerstner E 2007 *Nature* **446** 16
[8] Maine P, Strickland D, Bado P, Pessot M and Mourou G 1988 *IEEE J. Quantum Electron.* **24** 398
[9] Weber S, Bechet S, Borneis S *et al.* 2017 *Matter and Radiation at Extreme* **2** 149
[10] Malkin V M, Shvets G and Fisch N J 1999 *Phys. Rev. Lett.* **82** 4448
[11] Toroker Z, Malkin V M and Fisch N J 2012 *Phys. Rev. Lett.* **109** 085003
[12] Mourou G A, Fisch N J, Malkin V M, Toroker Z, Khazanov E A, Sergeev A M, Tajima T and Le Garrec B 2012 *Opt. Commun.* **285** 720
[13] Tajima T and Mourou G 2002 *Phys. Rev. ST Accel. Beams* **5** 031301
[14] Mourou G, Mironov S, Khazanov E and Sergeev A 2014 *Eur. Phys. J. Spec. Top.* **223** 1181
[15] Tolman R C, Ehrenfest P and Podolsky B 1931 *Phys. Rev.* **37** 602
[16] Scully M O 1979 *Phys. Rev. D* **19** 3582
[17] Ng K S and Raymond Ooi C H 2013 *Laser Phys.* **23** 035003
[18] Bonnor W B 1969 *Commun. Math. Phys.* **13** 163
[19] Rätzel D, Wilkens M and Menzel R 2016 *New J. Phys.* **18** 023009
[20] Schneiter F, Rätzel D and Braun D 2019 *Class. Quantum Gravity* **36** 119501
[21] Rätzel D and Fuentes I 2019 *J. Phys. Commun.* **3** 025009
[22] Flanagan É É and Hughes S A 2005 *New J. Phys.* **7** 204
[23] Arfken G B and Weber H J 2011 *Mathematical Methods for Physicists* (Amsterdam: Elsevier Academic Press)
[24] Bao W and Cai Y 2013 *Kinet. Relat. Models* **6** 1
[25] Di Nicola J M 2018 *Nucl. Fusion* **59** 032004
[26] Jourdain N, Chaulagain U, Havlik M, Kramer D, Kumar D, Majerova I, Tikhonchuk V, Korn G and Weber S 2021 *Matter and Radiation at Extreme* **6** 015401
[27] Ji P and Bai Y 2006 *Eur. Phys. J. C* **46** 817
[28] Sabín C, Bruschi D E, Ahmadi M and Fuentes I 2014 *New J. Phys.* **16** 085003
[29] Rätzel D, Howl R, Lindkvist J and Fuentes I 2018 *New J. Phys.* **20** 073044
[30] Altin P A, McDonald G, Dring D, Debs J E, Barter T H, Robins N P, Close J D, Haine S A, Hanna T M and Anderson R P 2011 *New J. Phys.* **13** 119401
[31] Szigeti S S, Nolan S P, Close J D and Haine S A 2020 *Phys. Rev. Lett.* **125** 100402
[32] Gupta S, Leanhardt A E, Cronin A D, Pritchard D E and Acad C R 2001 *Comptes Rendus de l'Academie des Sciences-Series IV: Physics, Astrophysics* **2** 479
[33] Gupta S, Dieckmann K, Hadzibabic Z and Pritchard D E 2002 *Phys. Rev. Lett.* **89** 140401
[34] Vaishnav J, Ruseckas J, Clark C and Juzeliūnas G 2008 *Phys. Rev. Lett.* **101** 265302
[35] Goldman N, Juzeliūnas G, Öhberg P and Spielman I 2014 *Rep. Prog. Phys.* **77** 126401
[36] Vaishnav J Y and Clark C W 2008 *Phys. Rev. Lett.* **100** 153002
[37] Jacob A, Öhberg P, Juzeliūnas G and Santos L 2007 *Appl. Phys. B* **89** 439
[38] Ramachandhran B, Opanchuk B, Liu X J, Pu H, Drummond P D and Hu H 2012 *Phys. Rev. A* **85** 023606
[39] Manchon A, Koo H C, Nitta J, Frolov S M and Duine R A 2015 *Nature Mater.* **14** 871
[40] Dowling J 1998 *Phys. Rev. A* **57** 4736
[41] Jamison A, Kutz J and Gupta S 2011 *Phys. Rev. A* **84** 043643
[42] Caves C M 1981 *Phys. Rev. D* **23** 1693
[43] Yurke B, McCall S L and Klauder J R 1986 *Phys. Rev. A* **33** 4033
[44] Huang Y and Hu Z D 2015 *Sci. Rep.* **5** 8006
[45] Huang X Y, Sun F X, Zhang W, He Q Y and Sun C P 2017 *Phys. Rev. A* **95** 013605
[46] Chen L, Zhang Y and Pu H 2020 *Phys. Rev. A* **102** 023317
[47] He Q Y, Vaughan T G, Drummond P D and Reid M D 2012 *New J. Phys.* **14** 093012
[48] Ma J, Wang X, Sun C and Nori F 2011 *Phys. Rep.* **509** 89
[49] Storey P and Cohen-Tannoudji C 1994 *Journal De Physique II* **4** 1999
[50] Fattori M, D'Errico C, Roati G, *et al.* 2008 *Phys. Rev. Lett.* **100** 080405
[51] Berrada T, van Frank S, Bücker R, Schumm T, Schaff J and Schmiedmayer J 2013 *Nat. Commun.* **4** 2077
[52] Butler A, Spence D J and Hooker S M 2002 *Phys. Rev. Lett.* **89** 185003
[53] Wen Q 2014 *Opt. Express* **22** 14782
[54] Spengler F, Rätzel D and Braun D 2022 *New J. Phys.* in press